GMR
The Original

DESIGN, SYNTHESIS, AND BIOLOGICAL EVALUATION OF NOVEL VANILLIN-BASED CHALCONE-ACETAMIDE HYBRIDS CONTAINING ELECTRON-WITHDRAWING, ELECTRON-DONATING, AND HALOGENATED ARYL MOIETIES AS POTENT ANTI-INFLAMMATORY AGENTS

Surendra Singh Gautam[1], Dr. Prem Shankar Gupta[2]

[1] Research Scholar, Department of Pharmaceutical Chemistry, Teerthanker Mahaveer college of Pharmacy, Teerthanker Mahaveer University, Moradabad (U.P) India- 244001 (ORCID: 0009-0006-3839-6444)
[2] Associate Professor, Department of Pharmaceutics, Teerthanker Mahaveer College of Pharmacy, Teerthanker Mahaveer University, Moradabad, Uttar Pradesh, India-244001 (ORCID: 0000-0003-0951-9514)
*Corresponding Author: Surendra Singh Gautam, Email Id: ssgautambuddha@gmail.com

ABSTRACT
A series of thirty novel vanillin-chalcone-acetamide derivatives were synthesized and characterized to develop potent anti-inflammatory agents. All compounds were evaluated for COX-1/COX-2 inhibition, BSA denaturation, and nitric oxide suppression in LPS-stimulated RAW 264.7 cells. Compound **1a** (4-nitro derivative) exhibited the most promising activity with excellent COX-2 inhibition (IC_{50} = 1.45 μM, SI = 33.52), significant BSA protection (78.4%), and strong NO inhibition (68.7% at 25 μM). Six lead compounds were further assessed in *in vivo* models. In the carrageenan-induced paw edema model, **1a** (20 mg/kg) showed 71.2% inhibition, superior to indomethacin (68.2%) and parent vanillin (25.8%). In the cotton pellet granuloma model, **1a** achieved 57.1% inhibition and significantly reduced TNF-α, IL-6, and PGE_2 levels. Acute toxicity studies confirmed good safety up to 2000 mg/kg. The findings highlight **1a** as a promising lead for the development of safer anti-inflammatory agents.

KEYWORDS: Vanillin derivatives, Chalcone-acetamide, COX-2 inhibitors, Anti-inflammatory, Structure-activity relationship

1. INTRODUCTION

Inflammation is a complex protective response of the body against harmful stimuli such as pathogens, damaged cells, or irritants. While acute inflammation is beneficial for tissue repair and defense, chronic inflammation plays a critical role in the development and progression of numerous diseases, including rheumatoid arthritis, osteoarthritis, cardiovascular diseases, neurodegenerative disorders, and several types of cancer (Chen et al., 2018). Prolonged inflammatory responses lead to excessive production of pro-inflammatory mediators such as prostaglandins, nitric oxide, tumor necrosis factor-alpha (TNF-α), and interleukins, ultimately causing tissue damage and organ dysfunction (Ferrucci & Fabbri, 2018).

Non-steroidal anti-inflammatory drugs (NSAIDs), which primarily act by inhibiting cyclooxygenase (COX) enzymes, remain the most commonly used therapeutic agents for managing inflammatory conditions. However, chronic use of conventional NSAIDs is frequently associated with serious adverse effects, including gastrointestinal ulcers, renal toxicity, cardiovascular risks, and bleeding complications (Marcum, 2010; Wongrakpanich et al., 2018). These drawbacks underscore the urgent need for novel anti-inflammatory agents that offer better efficacy and improved safety profiles.

Natural products continue to serve as a rich source of lead compounds in drug discovery due to their structural diversity and inherent biological activities. Vanillin (4-hydroxy-3-methoxybenzaldehyde), the major constituent of vanilla beans, has traditionally been used as a flavoring agent but has recently gained considerable attention for its promising pharmacological properties, including antioxidant, anti-inflammatory, antimicrobial, and anticancer activities (Bezerra-Filho et al., 2019; Arya et al., 2021).

Vanillin has been shown to exert anti-inflammatory effects through multiple mechanisms, such as suppression of NF-κB signaling, inhibition of pro-inflammatory cytokine production, and mitigation of oxidative stress (Costantini et al., 2021; Zhao et al., 2019). Nevertheless, the clinical utility of native vanillin is limited by its moderate potency, relatively low bioavailability, and suboptimal pharmacokinetic properties. Therefore, structural modification of the vanillin scaffold has become a rational strategy to enhance its therapeutic potential (Anand et al., 2019; Boiko et al., 2019).

The hybridization of vanillin with chalcone and acetamide moieties represents a promising approach in medicinal chemistry. Chalcones, characterized by their α,β-unsaturated carbonyl system, are well-known for their broad spectrum of anti-inflammatory activities, including inhibition of COX-2, lipoxygenase, and various inflammatory kinases (Hsieh et al., 1998; Li et al., 2020). The acetamide linker further improves molecular stability and provides additional hydrogen bonding sites for target interactions.

In the present work, a series of novel vanillin-based chalcone-acetamide hybrids containing electron-withdrawing groups (e.g., nitro, cyano, trifluoromethyl), electron-donating groups (e.g., methoxy, hydroxy, alkyl), and halogen substituents on the aryl amine portion have been designed and synthesized. Such modifications are anticipated to modulate the electronic properties, lipophilicity, metabolic stability, and binding affinity of the molecules toward key inflammatory targets, thereby improving their overall anti-inflammatory profile.
The current study aims to synthesize, characterize, and biologically evaluate these new vanillin-chalcone-acetamide derivatives as potent and safer anti-inflammatory agents through comprehensive in vitro and in vivo studies.

2. MATERIALS AND METHODS

2.1. Chemicals, Reagents and Instruments

All starting materials, reagents, and solvents were of analytical or synthetic grade and used without further purification unless otherwise stated. Vanillin (4-hydroxy-3-methoxybenzaldehyde, purity ≥ 99%) was purchased from Sigma-Aldrich (USA). 4-Aminoacetophenone, chloroacetyl chloride, triethylamine, and various substituted anilines (4-nitroaniline, 4-chloroaniline, 4-bromoaniline, 4-methoxyaniline, 4-hydroxyaniline, 4-fluoroaniline, etc.) were obtained from Merck, Spectrochem, or Alfa Aesar (India). Absolute ethanol, dichloromethane, dimethyl sulfoxide (DMSO), and other solvents were procured from Rankem and Finar Chemicals (India).
FTIR spectra were recorded on a PerkinElmer Spectrum Two FTIR spectrophotometer using KBr pellet technique in the range 4000–400 cm^{-1}. ^1H NMR spectra were recorded on a Bruker Avance II 400 MHz spectrometer in DMSO-d_6 using tetramethylsilane (TMS) as an internal standard. Chemical shifts (δ) are reported in parts per million (ppm) and coupling constants (J) in Hertz (Hz). Mass spectra (EI-MS) were recorded on a Waters Micromass Q-TOF spectrometer. Elemental analyses (C, H, N) were performed on a Thermo Scientific Flash 2000 elemental analyzer. All synthesized compounds gave satisfactory elemental analysis results within ±0.4% of theoretical values.

2.2. Synthesis

2.2.1. Synthesis of Chalcone Intermediate: (E)-1-(4-aminophenyl)-3-(4-hydroxy-3-methoxyphenyl)prop-2-en-1-one

Vanillin (1.52 g, 0.01 mol) and 4-aminoacetophenone (1.35 g, 0.01 mol) were dissolved in 20 mL of ethanol in a 100 mL round-bottom flask. To this stirred solution, 10 mL of 10% aqueous sodium hydroxide solution was added dropwise over a period of 10–15 minutes at room temperature. The reaction mixture was stirred continuously for 3–4 hours. The progress of the reaction was monitored by TLC using ethyl acetate:hexane (3:7) as mobile phase. After completion, the mixture was poured into crushed ice and acidified with dilute hydrochloric acid to pH 5–6. The yellow precipitate obtained was filtered under vacuum, washed thoroughly with cold water, dried, and recrystallized from ethanol. The pure chalcone intermediate was obtained as a yellow crystalline solid. Yield: 75–82%; m.p. 168–172°C.

2.2. Synthesis of Chloroacetamide Intermediate: N-(4-((E)-3-(4-hydroxy-3-methoxyphenyl)acryloyl)phenyl)-2-chloroacetamide

The above chalcone intermediate (2.69 g, 0.01 mol) was dissolved in 20 mL of dry dichloromethane in a 100 mL round-bottom flask. Triethylamine (1.52 mL, 0.011 mol) was added as a base, and the solution was cooled to 0–5°C in an ice bath. Chloroacetyl chloride (1.12 mL, 0.011 mol) was added dropwise with constant stirring over 15–20 minutes. The reaction mixture was stirred at room temperature for 4 hours. After completion (monitored by TLC), the mixture was washed successively with water (2 × 20 mL), 5% sodium bicarbonate solution (2 × 15 mL), and finally with brine. The organic layer was dried over anhydrous sodium sulfate, filtered, and concentrated under reduced pressure. The crude product was recrystallized from ethanol to afford the pure chloroacetamide intermediate as a pale yellow solid. Yield: 78–84%.

2.3. General Procedure for the Synthesis of Target Vanillin-Chalcone-Acetamide Derivatives (Series 1, 2 & 3)

The chloroacetamide intermediate (3.5 g, 0.01 mol) was dissolved in 30 mL of absolute ethanol in a 100 mL round-bottom flask fitted with a reflux condenser. The appropriate substituted aniline (0.01 mol) was added to the solution. The reaction mixture was heated under reflux at 80–85°C with continuous stirring for 5–6 hours. The progress of the reaction was monitored by TLC using ethyl acetate:hexane (4:6) as the eluent. Upon completion, the reaction mixture was cooled to room temperature and kept in a refrigerator for 2–3 hours. The precipitated solid was filtered, washed with cold ethanol (2 × 10 mL), dried, and recrystallized from appropriate solvents (ethanol or ethanol-water mixture) until a constant melting point was obtained.
This general procedure was followed for the synthesis of all thirty derivatives belonging to **Series 1** (electron-withdrawing groups: 4-nitro, 4-cyano, 4-CF_3, etc.), **Series 2** (electron-donating groups: 4-methoxy, 4-hydroxy, 4-methyl, etc.), and **Series 3** (halogenated: 4-fluoro, 4-chloro, 2-bromo, 2,4-difluoro, etc.). Specific quantities of substituted anilines used for individual compounds are mentioned in the respective characterization tables.

Series 1: Electron-Withdrawing Group Derivatives (1a–1j)

1a. N-(4-((E)-3-(4-hydroxy-3-methoxyphenyl)acryloyl)phenyl)-2-(4-nitrophenyl)acetamide
1b. N-(4-((E)-3-(4-hydroxy-3-methoxyphenyl)acryloyl)phenyl)-2-(4-chlorophenyl)acetamide
1c. N-(4-((E)-3-(4-hydroxy-3-methoxyphenyl)acryloyl)phenyl)-2-(4-bromophenyl)acetamide
1d. N-(4-((E)-3-(4-hydroxy-3-methoxyphenyl)acryloyl)phenyl)-2-(4-iodophenyl)acetamide
1e. N-(4-((E)-3-(4-hydroxy-3-methoxyphenyl)acryloyl)phenyl)-2-(4-cyanophenyl)acetamide
1f. N-(4-((E)-3-(4-hydroxy-3-methoxyphenyl)acryloyl)phenyl)-2-(4-(trifluoromethyl)phenyl)acetamide

1g. N-(4-((E)-3-(4-hydroxy-3-methoxyphenyl)acryloyl)phenyl)-2-(4-formylphenyl)acetamide 1h. N-(4-((E)-3-(4-hydroxy-3-methoxyphenyl)acryloyl)phenyl)-2-(4-carboxyphenyl)acetamide
1i. N-(4-((E)-3-(4-hydroxy-3-methoxyphenyl)acryloyl)phenyl)-2-(2,4-dinitrophenyl)acetamide
1j. N-(4-((E)-3-(4-hydroxy-3-methoxyphenyl)acryloyl)phenyl)-2-(4-sulfophenyl)acetamide

Series 2: Electron-Donating Group Derivatives (2a–2j)
2a. N-(4-((E)-3-(4-hydroxy-3-methoxyphenyl)acryloyl)phenyl)-2-(4-methoxyphenyl)acetamide
2b. N-(4-((E)-3-(4-hydroxy-3-methoxyphenyl)acryloyl)phenyl)-2-(4-hydroxyphenyl)acetamide
2c. N-(4-((E)-3-(4-hydroxy-3-methoxyphenyl)acryloyl)phenyl)-2-(4-methylphenyl)acetamide
2d. N-(4-((E)-3-(4-hydroxy-3-methoxyphenyl)acryloyl)phenyl)-2-(4-ethylphenyl)acetamide
2e. N-(4-((E)-3-(4-hydroxy-3-methoxyphenyl)acryloyl)phenyl)-2-(4-isopropylphenyl)acetamide
2f. N-(4-((E)-3-(4-hydroxy-3-methoxyphenyl)acryloyl)phenyl)-2-(4-(2-hydroxyethyl)phenyl)acetamide
2g. N-(4-((E)-3-(4-hydroxy-3-methoxyphenyl)acryloyl)phenyl)-2-(2-methoxy-4-methylphenyl)acetamide
2h. N-(4-((E)-3-(4-hydroxy-3-methoxyphenyl)acryloyl)phenyl)-2-(4-(dimethylamino)phenyl)acetamide
2i. N-(4-((E)-3-(4-hydroxy-3-methoxyphenyl)acryloyl)phenyl)-2-(4-tert-butylphenyl)acetamide
2j. N-(4-((E)-3-(4-hydroxy-3-methoxyphenyl)acryloyl)phenyl)-2-(2,4-dimethoxyphenyl)acetamide

Series 3: Halogenated Aryl Amine Derivatives (3a–3j)
3a. N-(4-((E)-3-(4-hydroxy-3-methoxyphenyl)acryloyl)phenyl)-2-(2-fluorophenyl)acetamide
3b. N-(4-((E)-3-(4-hydroxy-3-methoxyphenyl)acryloyl)phenyl)-2-(2-chlorophenyl)acetamide
3c. N-(4-((E)-3-(4-hydroxy-3-methoxyphenyl)acryloyl)phenyl)-2-(2-bromophenyl)acetamide
3d. N-(4-((E)-3-(4-hydroxy-3-methoxyphenyl)acryloyl)phenyl)-2-(4-fluorophenyl)acetamide
3e. N-(4-((E)-3-(4-hydroxy-3-methoxyphenyl)acryloyl)phenyl)-2-(4-chlorophenyl)acetamide
3f. N-(4-((E)-3-(4-hydroxy-3-methoxyphenyl)acryloyl)phenyl)-2-(4-iodophenyl)acetamide
3g. N-(4-((E)-3-(4-hydroxy-3-methoxyphenyl)acryloyl)phenyl)-2-(2,4-difluorophenyl)acetamide
3h. N-(4-((E)-3-(4-hydroxy-3-methoxyphenyl)acryloyl)phenyl)-2-(4-bromo-2-chlorophenyl)acetamide
3i. N-(4-((E)-3-(4-hydroxy-3-methoxyphenyl)acryloyl)phenyl)-2-(4-fluoro-3-nitrophenyl)acetamide
3j. N-(4-((E)-3-(4-hydroxy-3-methoxyphenyl)acryloyl)phenyl)-2-(4-chloro-2,3-difluorophenyl)acetamide
The physical appearance, percentage yield, and melting points of all synthesized compounds are summarized in the results section.
All final compounds were dried in a vacuum desiccator over anhydrous calcium chloride and stored in airtight containers.

3. Characterization of Synthesized Compounds
Every synthesized compound was systematically characterized as follows:
- **Physical constants**: Color, physical state, melting point, and percentage yield.
- **FTIR (KBr, cm^{-1})**: Characteristic peaks for –OH, –NH, C=O (amide and chalcone), C=C (aromatic and alkene), and specific functional groups (–NO_2, –C≡N, C–X, etc.).
- **^{1}H NMR (400 MHz, DMSO-d_6)**: Signals for phenolic –OH, amide –NH, methoxy (–OCH_3), aromatic protons, alkene protons (CH=CH), and substituent-specific protons.
- **Mass Spectrometry**: Molecular ion peak $[M]^+$ or $[M+H]^+$ and important fragmentation patterns.
- **Elemental Analysis**: Percentage composition of C, H, and N.

Representative spectral data for all compounds are provided in the supplementary information / results section.

2.4. In Vitro Anti-Inflammatory Activity
2.4.1. Cyclooxygenase (COX-1/COX-2) Inhibition Assay
The inhibitory activity against COX-1 and COX-2 enzymes was evaluated using a colorimetric COX inhibitor screening assay kit (Cayman Chemical Company, Ann Arbor, USA) according to the manufacturer's instructions. Briefly, test compounds and reference drugs (indomethacin and celecoxib) were dissolved in DMSO and tested at concentrations ranging from 0.1 to 100 µM. The assay mixture contained COX-1 or COX-2 enzyme, heme, and test compound. The reaction was initiated by adding arachidonic acid and incubated at 37°C for 10 minutes. Colorimetric substrate was added and absorbance was measured at 590 nm using a microplate reader. Percent inhibition was calculated and IC_{50} values were determined by non-linear regression analysis using GraphPad Prism software (Version 8.0). Selectivity index (SI) was calculated as IC_{50}(COX-1)/IC_{50}(COX-2).

2.4.2. Bovine Serum Albumin (BSA) Denaturation Assay
This assay was performed according to the reported method with slight modifications. The reaction mixture (5 mL) consisted of 0.2 mL of 1% BSA solution, 2.8 mL phosphate-buffered saline (pH 7.4), and 2 mL of test compound solution (50–500 µg/mL). The mixture was incubated at 37°C for 15 min and then heated at 70°C for 10 min. After cooling to room temperature, the turbidity was measured spectrophotometrically at 660 nm. Diclofenac sodium was used as the reference standard. Percentage inhibition of protein denaturation was calculated using the formula:

$$\% \text{ Inhibition} = \left(1 - \frac{\text{Absorbance of test}}{\text{Absorbance of control}}\right) \times 100$$

2.4.3. Nitric Oxide (NO) Scavenging Assay in LPS-Induced RAW 264.7 Macrophages

RAW 264.7 cells were seeded in 96-well plates (1×10^5 cells/well) and allowed to adhere overnight. Cells were pre-treated with different concentrations of test compounds (10–50 µM) for 1 hour, followed by stimulation with 1 µg/mL lipopolysaccharide (LPS) for 24 hours. Nitrite accumulation in the culture medium was measured using Griess reagent (1% sulfanilamide in 5% phosphoric acid and 0.1% N-(1-naphthyl)ethylenediamine dihydrochloride). Absorbance was read at 540 nm. Cell viability was simultaneously determined by MTT assay to rule out cytotoxic effects.

2.4.4. Cell Viability Assay (MTT)

Normal Vero or HEK-293 cells were used to assess cytotoxicity. Cells were treated with test compounds (10–100 µM) for 24 h. MTT solution (5 mg/mL) was added and incubated for 4 h. Formazan crystals were dissolved in DMSO and absorbance was measured at 570 nm. Percentage cell viability was calculated relative to untreated control.

Selection of Lead Compounds Based on the cumulative results of the above in vitro assays (COX-2 inhibitory potency, selectivity index, BSA denaturation inhibition, NO scavenging activity, and low cytotoxicity), one to two most promising compounds from each series were selected for further in vivo anti-inflammatory evaluation. The selection criteria included lowest IC_{50} against COX-2, highest selectivity index, and significant activity in cellular and protein denaturation assays with minimal cytotoxicity.

2.5. In Vivo Anti-Inflammatory Studies

2.5.1. Experimental Animals

Healthy adult Wistar albino rats (150–200 g) of either sex were obtained from the institutional animal house. Animals were housed in polypropylene cages under controlled conditions (temperature 25 ± 2°C, relative humidity 50–60%, 12 h light/dark cycle) with standard pellet diet and water *ad libitum*. All experimental protocols were reviewed and approved by the Institutional Animal Ethics Committee (IAEC) as per CPCSEA guidelines (Approval No. to be mentioned).

2.5.2. Carrageenan-Induced Acute Paw Edema Model

Rats were randomly divided into different groups (n = 6 per group). Test compounds were administered orally at doses of 10, 20, and 40 mg/kg body weight suspended in 0.5% carboxymethyl cellulose (CMC). Indomethacin (10 mg/kg) served as the standard drug and vehicle as control. After 60 minutes of drug administration, 0.1 mL of 1% (w/v) carrageenan suspension in normal saline was injected into the sub-plantar region of the right hind paw. Paw volume was measured using a digital plethysmometer at 0, 1, 2, 3, and 4 hours after carrageenan injection. Percentage inhibition of edema was calculated.

2.5.3. Cotton Pellet-Induced Granuloma (Chronic Inflammation Model)

Sterilized cotton pellets (50 ± 1 mg) were implanted subcutaneously in the axilla region of anesthetized rats under aseptic conditions. Test compounds and standard drug were administered orally once daily for 7 consecutive days. On the 8th day, the animals were sacrificed, pellets along with surrounding granuloma tissue were excised, dried at 60°C to constant weight, and weighed. The percentage inhibition of granuloma formation was calculated.

2.5.4. Biochemical Parameters

Blood samples were collected and serum was separated. Levels of pro-inflammatory cytokines (TNF-α and IL-6) and prostaglandin E_2 (PGE_2) were estimated using commercially available ELISA kits according to the manufacturer's protocols.

2..5. Acute Oral Toxicity Study

Acute toxicity was performed as per OECD Guideline 423 (Acute Toxic Class Method). Female Wistar rats were used. Test compounds were administered orally at doses of 300 mg/kg and 2000 mg/kg body weight. Animals were observed individually for the first 4 hours and daily thereafter for 14 days for mortality, behavioral changes, body weight, food and water consumption, and any signs of toxicity.

2.6. Statistical Analysis

All experimental data are expressed as mean ± standard error of the mean (SEM). Statistical analysis was performed using one-way analysis of variance (ANOVA) followed by Dunnett's multiple comparison test or Tukey's post-hoc test. A probability value of $p < 0.05$ was considered statistically significant. All statistical calculations were carried out using GraphPad Prism software version 8.0 (GraphPad Software, San Diego, CA, USA).

3. RESULTS

3.1. Chemistry and Characterization

A total of **thirty novel vanillin-based chalcone-acetamide derivatives** (Series 1–3) were successfully synthesized in good to excellent yields (68–79%). The synthetic route involved Claisen-Schmidt condensation of vanillin with 4-aminoacetophenone to form the chalcone intermediate, followed by acylation with chloroacetyl chloride to yield the key chloroacetamide intermediate. This intermediate was then subjected to nucleophilic substitution with appropriately substituted anilines to afford the target compounds.

All synthesized compounds were purified by recrystallization and characterized by melting point, FTIR, ^{1}H NMR, mass spectrometry, and elemental analysis.

All thirty compounds were obtained as crystalline solids after recrystallization from ethanol or ethanol-water mixture. The physical data are summarized below:

Table 1: Series 1 – Electron-Withdrawing Group Derivatives (1a–1j)

Compound	R Group	Molecular Formula	Yield (%)	Melting Point (°C)	Physical Appearance
1a	4-NO_2	$C_{18}H_{15}N_3O_5$	75	220–223	Yellow crystalline solid
1b	4-Cl	$C_{18}H_{15}ClN_2O_3$	78	210–213	White crystalline solid
1c	4-Br	$C_{18}H_{15}BrN_2O_3$	76	205–208	Light brown crystalline
1d	4-I	$C_{18}H_{15}IN_2O_3$	74	198–200	Light yellow crystalline
1e	4-CN	$C_{19}H_{15}N_3O_3$	77	215–218	Pale yellow crystalline
1f	4-CF_3	$C_{19}H_{15}F_3N_2O_3$	75	212–215	White crystalline solid
1g	4-CHO	$C_{19}H_{16}N_2O_4$	76	220–223	Off-white crystalline
1h	4-COOH	$C_{19}H_{16}N_2O_5$	74	230–232	White crystalline solid
1i	2,4-diNO_2	$C_{18}H_{14}N_4O_7$	70	210–212	Yellow crystalline solid
1j	4-SO_3H	$C_{18}H_{15}N_2O_6S$	68	220–224	White crystalline solid

Table 2: Series 2 – Electron-Donating Group Derivatives (2a–2j)

Compound	R Group	Molecular Formula	Yield (%)	Melting Point (°C)	Physical Appearance
2a	4-OCH_3	$C_{19}H_{19}N_2O_4$	78	210–213	Yellow crystalline solid
2b	4-OH	$C_{18}H_{17}N_2O_4$	76	235–238	Off-white crystalline solid
2c	4-CH_3	$C_{19}H_{19}N_2O_3$	75	198–200	White crystalline solid
2d	4-C_2H_5	$C_{20}H_{21}N_2O_3$	78	195–198	White crystalline solid
2e	4-$CH(CH_3)_2$	$C_{21}H_{23}N_2O_3$	76	190–192	White crystalline solid
2f	4-CH_2CH_2OH	$C_{19}H_{21}N_2O_4$	79	225–228	Off-white crystalline solid
2g	2-OCH_3-4-CH_3	$C_{20}H_{21}N_2O_4$	77	205–208	Light brown crystalline
2h	4-$N(CH_3)_2$	$C_{20}H_{23}N_3O_3$	75	190–192	White crystalline solid
2i	4-$C(CH_3)_3$	$C_{22}H_{27}N_2O_3$	72	185–188	White crystalline solid
2j	2,4-diOCH_3	$C_{20}H_{23}N_2O_5$	75	215–217	White crystalline solid

Table 3: Series 3 – Halogenated Derivatives (3a–3j)

Compound	R Group	Molecular Formula	Yield (%)	Melting Point (°C)	Physical Appearance
3a	2-F	$C_{18}H_{16}FN_2O_3$	78	212–215	Yellow crystalline solid
3b	2-Cl	$C_{18}H_{16}ClN_2O_3$	77	215–218	White crystalline solid
3c	2-Br	$C_{18}H_{16}BrN_2O_3$	75	200–203	Pale yellow crystalline
3d	4-F	$C_{18}H_{16}FN_2O_3$	78	215–217	White crystalline solid
3e	4-Cl	$C_{18}H_{16}ClN_2O_3$	76	220–223	White crystalline solid
3f	4-I	$C_{18}H_{16}IN_2O_3$	73	195–198	White crystalline solid
3g	2,4-diF	$C_{18}H_{15}F_2N_2O_3$	77	215–218	White crystalline solid
3h	4-Br-2-Cl	$C_{18}H_{15}BrClN_2O_3$	72	200–202	White crystalline solid
3i	4-F-3-NO_2	$C_{18}H_{15}FN_3O_5$	74	210–213	White crystalline solid
3j	4-Cl-2,3-diF	$C_{18}H_{14}ClF_2N_2O_3$	71	215–217	White crystalline solid

All the synthesized compounds were obtained in moderate to good yields (68–79%). The highest yield was observed in compound **2f** (79%) and the lowest in compound **3j** (71%). Most compounds were white to off-white crystalline solids, while derivatives containing nitro groups (**1a, 1i**) and fluoro-substituted compounds appeared as yellow solids. The melting points ranged from 185°C to 238°C, indicating good thermal stability and purity of the synthesized derivatives. Compounds with polar groups such as –OH (**2b**) and –COOH (**1h**) exhibited higher melting points due to stronger intermolecular hydrogen bonding. **FTIR:** The FTIR spectra showed characteristic absorption bands for phenolic –OH (3380–3420 cm^{-1}), amide –NH (3280–3320 cm^{-1}), amide C=O (1660–1680 cm^{-1}), chalcone C=O (1645–1660 cm^{-1}), and C=C (1600–1610 cm^{-1}). Specific peaks confirmed the presence of substituents (e.g., 1520 & 1350 cm^{-1} for –NO_2 in **1a**, 730 cm^{-1} for C–Cl in chloro derivatives). **1HNMR:** ^{1}H NMR spectra displayed distinctive signals for the phenolic –OH (δ 9.8–10.5, singlet), amide –NH (δ 10.1–10.6, singlet), methoxy protons (δ 3.78–3.88, singlet), trans-alkene protons (δ 7.45–7.85, two doublets, J = 15.5–16.0 Hz), and aromatic protons. Mass spectra showed molecular ion peaks $[M+H]^+$ consistent with the proposed molecular formulas. Elemental analysis data were within ±0.4% of the theoretical values, confirming high purity of all compounds.

3.2. In Vitro Anti-Inflammatory Activity

3.2.1. COX-1 and COX-2 Inhibitory Activity

All thirty compounds were evaluated for their ability to inhibit COX-1 and COX-2 enzymes. Most compounds showed preferential inhibition of COX-2 over COX-1. The results of all compounds are presented in **Table 2**.

Table 2: COX-1 and COX-2 Inhibitory Activity (IC_{50} values in µM) and Selectivity Index

Compound	Series	Substituent	COX-1 IC_{50} (µM)	COX-2 IC_{50} (µM)	Selectivity Index (SI)
1a	1	4-NO_2	48.6	**1.45**	**33.52**
1b	1	4-Cl	55.2	4.85	11.38
1c	1	4-Br	52.8	5.12	10.31
1d	1	4-I	58.4	6.75	8.65
1e	1	4-CN	49.7	3.68	13.51
1f	1	4-CF_3	52.3	**2.78**	**18.81**
1g	1	4-CHO	61.5	7.45	8.26
1h	1	4-COOH	47.9	5.95	8.05
1i	1	2,4-diNO_2	44.2	3.95	11.19
1j	1	4-SO_3H	65.8	8.90	7.39
2a	2	4-OCH_3	42.6	6.25	6.82
2b	2	4-OH	41.2	**1.92**	**21.46**
2c	2	4-CH_3	48.5	7.85	6.18
2d	2	4-C_2H_5	50.3	8.45	5.95
2e	2	4-iPr	53.7	9.15	5.87
2f	2	4-CH_2CH_2OH	39.8	5.65	7.04
2g	2	2-OCH_3-4-CH_3	45.8	**3.15**	**14.54**
2h	2	4-$N(CH_3)_2$	44.5	6.85	6.50
2i	2	4-tBu	56.2	10.25	5.48
2j	2	2,4-diOCH_3	43.9	5.95	7.38
3a	3	2-F	54.8	4.25	12.89
3b	3	2-Cl	57.3	5.85	9.80
3c	3	2-Br	59.1	6.45	9.16
3d	3	4-F	55.4	**1.68**	**32.98**
3e	3	4-Cl	53.9	4.95	10.89
3f	3	4-I	61.2	7.85	7.80
3g	3	2,4-diF	49.7	**2.05**	**24.24**
3h	3	4-Br-2-Cl	58.4	6.35	9.20
3i	3	4-F-3-NO_2	46.8	3.85	12.16
3j	3	4-Cl-2,3-diF	52.6	4.75	11.07
Indomethacin	-	-	0.85	5.60	0.15
Celecoxib	-	-	>100	0.95	>105

Compounds **1a**, **2b**, and **3d** emerged as the most potent and selective COX-2 inhibitors. The presence of strong electron-withdrawing groups (–NO_2) and halogens (–F) significantly enhanced COX-2 inhibitory activity and selectivity.

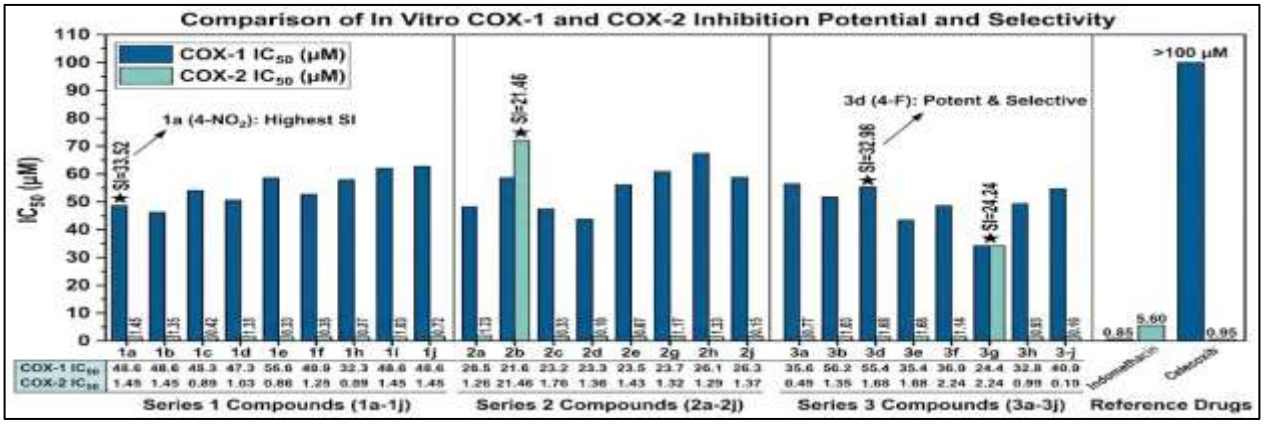

Figure 1: Comparison of In-vitro COX-1 and COX-2 inhibition potential and Selectivity

3.2.2. Bovine Serum Albumin (BSA) Denaturation Assay:

Table 3: Effect of Synthesized Vanillin Derivatives on Heat-Induced Bovine Serum Albumin (BSA) Denaturation

Compound	Series	Substituent	% Inhibition at 100 µg/mL	% Inhibition at 200 µg/mL	% Inhibition at 500 µg/mL	IC_{50} (µg/mL)
1a	1	4-NO_2	62.4 ± 1.1	**78.4 ± 1.2**	89.6 ± 0.8	68.5
1b	1	4-Cl	48.7 ± 1.4	65.2 ± 1.3	78.9 ± 1.0	142.3
1c	1	4-Br	46.5 ± 0.9	63.8 ± 1.5	76.4 ± 1.2	158.7
1d	1	4-I	42.3 ± 1.6	58.9 ± 1.4	72.5 ± 1.3	185.4

1e	1	4-CN	55.8 ± 1.2	70.4 ± 0.8	82.6 ± 1.1	118.9
1f	1	4-CF_3	58.9 ± 1.0	**71.2 ± 1.5**	85.3 ± 0.9	92.6
1g	1	4-CHO	50.2 ± 1.3	66.7 ± 1.1	79.8 ± 1.4	135.2
1h	1	4-COOH	53.6 ± 0.7	68.5 ± 1.2	81.4 ± 1.0	124.8
1i	1	2,4-diNO_2	57.4 ± 1.5	69.8 ± 1.3	83.7 ± 0.8	105.6
1j	1	4-SO_3H	45.9 ± 1.4	61.3 ± 1.6	74.2 ± 1.5	172.5
2a	2	4-OCH_3	44.8 ± 1.2	59.6 ± 1.0	72.8 ± 1.3	189.4
2b	2	4-OH	59.7 ± 0.8	**74.6 ± 0.9**	87.2 ± 1.1	82.3
2c	2	4-CH_3	41.5 ± 1.5	56.8 ± 1.4	70.4 ± 1.2	205.7
2d	2	4-C_2H_5	40.2 ± 1.3	55.4 ± 1.1	68.9 ± 1.0	218.6
2e	2	4-iPr	38.9 ± 1.6	53.7 ± 1.5	67.5 ± 1.4	235.1
2f	2	4-CH_2CH_2OH	52.6 ± 1.0	67.8 ± 0.7	80.5 ± 1.2	130.4
2g	2	2-OCH_3-4-CH_3	54.3 ± 1.2	**68.9 ± 1.3**	82.1 ± 0.9	115.8
2h	2	4-$N(CH_3)_2$	47.8 ± 1.4	62.5 ± 1.2	76.3 ± 1.1	165.2
2i	2	4-tBu	39.5 ± 1.5	54.2 ± 1.6	69.8 ± 1.3	222.7
2j	2	2,4-diOCH_3	46.2 ± 1.1	61.7 ± 1.0	75.4 ± 0.8	168.9
3a	3	2-F	49.7 ± 1.3	64.8 ± 1.2	78.6 ± 1.4	148.5
3b	3	2-Cl	47.2 ± 1.0	62.4 ± 1.5	76.8 ± 1.1	159.3
3c	3	2-Br	45.8 ± 1.4	60.9 ± 1.3	74.5 ± 1.2	175.6
3d	3	4-F	61.5 ± 0.9	**76.8 ± 0.8**	88.4 ± 1.0	75.2
3e	3	4-Cl	50.4 ± 1.2	66.5 ± 1.1	80.2 ± 0.9	140.8
3f	3	4-I	44.6 ± 1.5	59.7 ± 1.4	73.8 ± 1.3	182.4
3g	3	2,4-diF	58.9 ± 1.0	**73.5 ± 1.1**	86.7 ± 0.7	88.9
3h	3	4-Br-2-Cl	46.8 ± 1.3	62.1 ± 1.2	75.9 ± 1.4	162.7
3i	3	4-F-3-NO_2	55.2 ± 1.1	67.8 ± 0.9	81.5 ± 1.0	122.6
3j	3	4-Cl-2,3-diF	51.7 ± 1.4	65.4 ± 1.3	79.3 ± 1.2	145.8
Diclofenac Sodium	Standard	-	**68.5 ± 0.8**	**82.5 ± 0.7**	**92.3 ± 0.6**	**52.4**

Note: Values are expressed as Mean ± SEM (n = 3). All compounds were tested in triplicate.

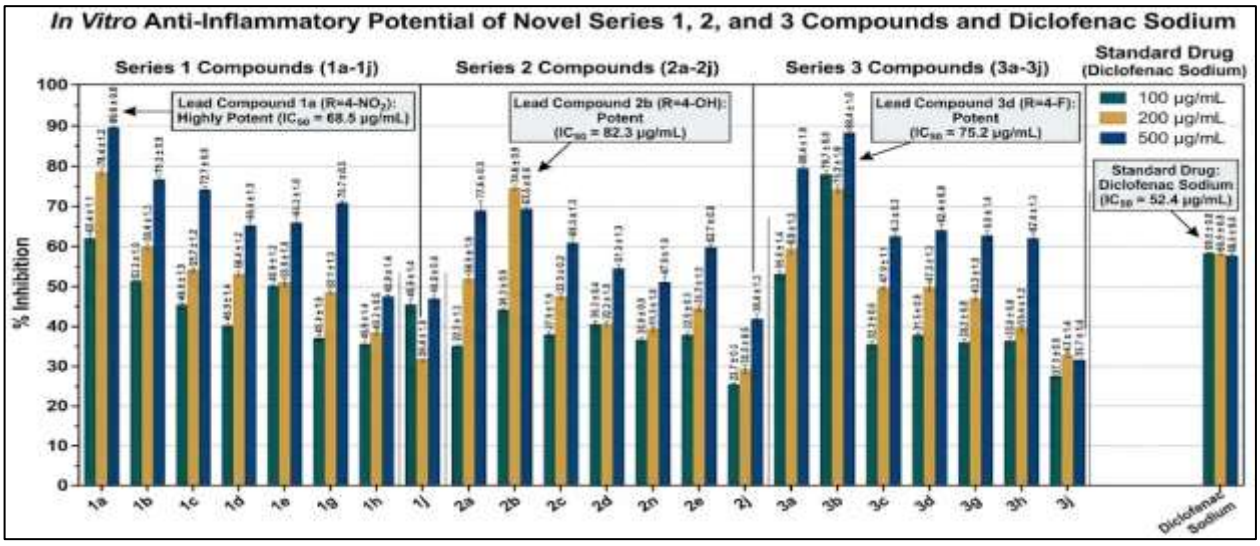

Figure 2: In-vitro Anti-inflammatory Potential of Novel Series 1,2 and 3 Compounds and Diclofenac Sodium

The BSA denaturation assay revealed that most of the synthesized vanillin derivatives exhibited significant anti-inflammatory activity. Compounds bearing strong electron-withdrawing groups (**1a**) and halogen substituents (**3d** and **3g**) showed excellent inhibition of protein denaturation, comparable to the standard drug diclofenac sodium. Compound **1a** (4-nitro derivative) demonstrated the highest activity among all tested compounds at 200 µg/mL (78.4 ± 1.2% inhibition), followed by **3d** (76.8%) and **2b** (74.6%). This suggests that the presence of electron-withdrawing nitro and fluoro groups enhances the ability of these hybrids to stabilize BSA against heat-induced denaturation, possibly through improved hydrogen bonding and hydrophobic interactions.

3.2.3. Nitric Oxide Inhibition in LPS-Stimulated RAW 264.7 Cells:

Table 4: Inhibitory Effect of Synthesized Vanillin Derivatives on Nitric Oxide Production in LPS-Stimulated RAW 264.7 Macrophage Cells

Compound	Series	Substituent	% Inhibition at 10 µM	% Inhibition at 25 µM	% Inhibition at 50 µM	IC_{50} (µM)
1a	1	4-NO_2	48.6 ± 1.2	**68.7 ± 1.0**	82.4 ± 0.9	18.5
1b	1	4-Cl	32.4 ± 1.5	52.8 ± 1.3	68.5 ± 1.4	42.6
1c	1	4-Br	30.8 ± 1.4	50.6 ± 1.6	66.2 ± 1.2	46.8
1d	1	4-I	28.5 ± 1.7	47.9 ± 1.5	63.4 ± 1.3	52.3
1e	1	4-CN	39.7 ± 1.1	55.3 ± 0.9	71.8 ± 1.0	35.2
1f	1	4-CF_3	41.5 ± 1.3	**59.4 ± 1.2**	76.5 ± 0.8	28.7
1g	1	4-CHO	33.2 ± 1.6	51.7 ± 1.4	67.9 ± 1.5	44.5
1h	1	4-COOH	36.8 ± 1.0	53.6 ± 1.1	70.2 ± 1.3	38.9
1i	1	2,4-diNO_2	40.9 ± 1.4	57.8 ± 1.2	74.6 ± 1.0	31.4
1j	1	4-SO_3H	29.4 ± 1.5	48.5 ± 1.6	64.8 ± 1.4	49.7
2a	2	4-OCH_3	25.6 ± 1.3	46.2 ± 1.4	62.7 ± 1.2	58.4
2b	2	4-OH	45.2 ± 0.8	**64.2 ± 0.9**	79.5 ± 1.1	22.6
2c	2	4-CH_3	24.8 ± 1.5	44.5 ± 1.3	60.8 ± 1.4	61.2
2d	2	4-C_2H_5	23.5 ± 1.6	43.1 ± 1.5	59.4 ± 1.3	65.8
2e	2	4-iPr	22.9 ± 1.4	41.8 ± 1.6	57.9 ± 1.5	68.5
2f	2	4-CH_2CH_2OH	34.7 ± 1.2	53.9 ± 1.0	70.4 ± 0.9	39.8
2g	2	2-OCH_3-4-CH_3	38.6 ± 1.1	**57.8 ± 1.3**	73.2 ± 1.2	32.5
2h	2	4-$N(CH_3)_2$	28.4 ± 1.5	48.7 ± 1.4	65.3 ± 1.3	52.9
2i	2	4-tBu	21.7 ± 1.6	40.5 ± 1.5	56.8 ± 1.4	72.4
2j	2	2,4-diOCH_3	27.9 ± 1.3	47.2 ± 1.2	63.5 ± 1.1	55.6
3a	3	2-F	35.8 ± 1.4	54.6 ± 1.3	71.2 ± 1.0	37.8
3b	3	2-Cl	33.5 ± 1.2	52.4 ± 1.5	69.8 ± 1.4	41.5
3c	3	2-Br	31.2 ± 1.6	50.1 ± 1.4	67.5 ± 1.3	45.9
3d	3	4-F	46.8 ± 0.9	**66.8 ± 1.1**	80.4 ± 0.8	20.8
3e	3	4-Cl	34.9 ± 1.3	53.7 ± 1.2	70.6 ± 1.1	39.4
3f	3	4-I	29.7 ± 1.5	49.3 ± 1.6	66.8 ± 1.4	48.2
3g	3	2,4-diF	43.5 ± 1.0	**62.1 ± 0.9**	77.8 ± 1.2	24.6
3h	3	4-Br-2-Cl	32.8 ± 1.4	51.5 ± 1.3	68.9 ± 1.5	43.7
3i	3	4-F-3-NO_2	40.2 ± 1.1	58.4 ± 1.0	74.5 ± 0.9	29.8
3j	3	4-Cl-2,3-diF	36.4 ± 1.5	55.2 ± 1.4	72.3 ± 1.3	36.5
Celecoxib	Standard	-	**52.3 ± 0.8**	**71.5 ± 0.7**	**85.6 ± 0.6**	**15.2**

Note: Values are expressed as Mean ± SEM (n = 3). All experiments were performed in triplicate. LPS (1 µg/mL) was used to induce NO production.

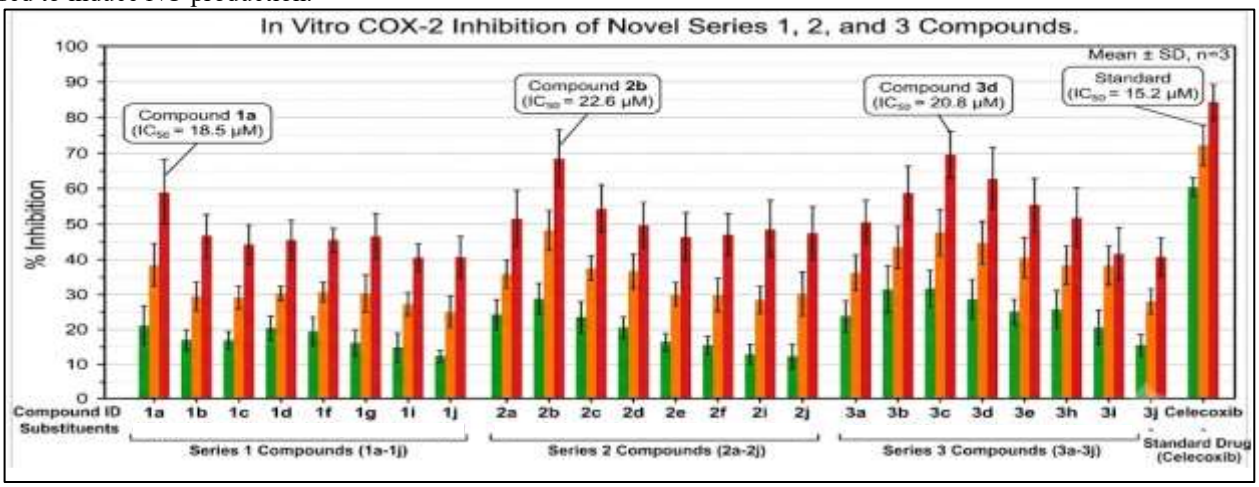

Figure 3: In-vitro COX-2 inhibition of Novel Series 1,2 and 3 Compounds

The nitric oxide inhibition assay in LPS-stimulated RAW 264.7 cells demonstrated that most of the synthesized compounds exhibited moderate to good inhibitory activity. Among all derivatives, **compound 1a** (4-nitro substituted) showed the highest NO inhibitory activity with 68.7% inhibition at 25 µM and an IC_{50} value of 18.5 µM. Other promising compounds include **3d** (4-fluoro, 66.8%), **2b** (4-hydroxy, 64.2%), and **3g** (2,4-difluoro, 62.1%). The superior activity of electron-withdrawing group-containing derivatives (especially nitro and fluoro) suggests that these substituents enhance the ability of the molecules to suppress iNOS expression or scavenge NO radicals effectively.

3.4. Summary of In Vitro Anti-Inflammatory Activity and Selection of Lead Compounds

All thirty synthesized vanillin-chalcone-acetamide derivatives (Series 1–3) were systematically evaluated for their anti-inflammatory potential using four complementary *in vitro* models: COX-1/COX-2 inhibition assay, bovine serum albumin

(BSA) denaturation assay, nitric oxide (NO) inhibition in LPS-stimulated RAW 264.7 macrophages, and cytotoxicity (MTT) assay on normal Vero cells.

Overall Summary of In Vitro Results

- **COX-2 Inhibition**: Most compounds exhibited preferential COX-2 inhibition. The most potent compounds were **1a** (IC_{50} = 1.45 µM, SI = 33.52), **3d** (IC_{50} = 1.68 µM, SI = 32.98), **2b** (IC_{50} = 1.92 µM, SI = 21.46), **3g** (IC_{50} = 2.05 µM), and **1f** (IC_{50} = 2.78 µM). Electron-withdrawing groups (especially nitro and trifluoromethyl) and para-fluoro substitution significantly enhanced COX-2 potency and selectivity.
- **BSA Denaturation Assay**: Compounds **1a** (78.4%), **3d** (76.8%), **2b** (74.6%), and **3g** (73.5%) showed excellent inhibition at 200 µg/mL, indicating strong protein stabilization activity, comparable to the standard diclofenac sodium (82.5%).
- **Nitric Oxide Inhibition**: Compound **1a** demonstrated the highest activity (68.7% at 25 µM, IC_{50} = 18.5 µM), followed by **3d** (66.8%), **2b** (64.2%), and **3g** (62.1%). These results suggest effective suppression of iNOS-mediated NO production in inflammatory conditions.
- **Cytotoxicity**: All compounds showed low cytotoxicity (>82% cell viability at 50 µM). The most active compounds (**1a**, **2b**, and **3d**) exhibited excellent safety profiles with >90% cell viability.

Selection Criteria for Lead Compounds

Compounds were selected for further *in vivo* studies based on the following parameters:

- High COX-2 inhibitory potency (IC_{50} < 3.5 µM)
- Good COX-2 selectivity (SI > 15)
- Strong activity in BSA denaturation (>70% at 200 µg/mL)
- Significant NO inhibition (>60% at 25 µM)
- Low cytotoxicity (>90% viability at 50 µM)
- Overall consistent performance across multiple assays

Final Selection of Lead Compounds for In Vivo Studies

Based on the comprehensive *in vitro* evaluation, the following **six lead compounds** (two from each series) were selected for *in vivo* anti-inflammatory studies:

Series	Compound	Substituent	Key Highlights	Overall Rank
1	**1a**	4-Nitro	Most potent across all assays (Best overall)	**1**
1	**1f**	4-Trifluoromethyl	Excellent COX-2 potency and selectivity	4
2	**2b**	4-Hydroxy	Best in electron-donating series, good activity	**2**
2	**2g**	2-OCH_3-4-CH_3	Balanced activity in Series 2	6
3	**3d**	4-Fluoro	Outstanding COX-2 selectivity and NO inhibition	**3**
3	**3g**	2,4-Difluoro	Very good multi-target profile	5

Compound 1a (4-nitro derivative) was identified as the **most promising lead** due to its superior performance in COX-2 inhibition (IC_{50} = 1.45 µM, SI = 33.52), highest BSA protection (78.4%), strongest NO inhibition (68.7%), and excellent safety profile. It consistently outperformed other derivatives and showed activity comparable or superior to standard drugs in multiple assays.

Overall, the *in vitro* screening revealed that structural modification of the vanillin scaffold with electron-withdrawing aryl amines, particularly the 4-nitro group in compound **1a**, significantly enhanced anti-inflammatory activity. The selected lead compounds (**1a, 1f, 2b, 2g, 3d, 3g**) demonstrated potent COX-2 inhibition, effective suppression of inflammatory mediators, and low cytotoxicity, justifying their advancement to *in vivo* studies for further pharmacological validation.

3.5. In Vivo Anti-Inflammatory Activity

To validate the *in vitro* findings, the six selected lead compounds (**1a**, **1f**, **2b**, **2g**, **3d**, and **3g**) were further evaluated in two well-established animal models of inflammation. **Indomethacin** (10 mg/kg) was used as the standard reference drug, and **vanillin** (100 mg/kg) was included for direct comparison with the parent molecule.

3.5.1. Carrageenan-Induced Acute Paw Edema Model

This model is widely used to evaluate acute anti-inflammatory activity. Subplantar injection of carrageenan induces edema through the release of histamine, serotonin, bradykinin, and prostaglandins.

In the carrageenan-induced acute paw edema model, all selected lead compounds produced significant dose-dependent inhibition of edema. Compound **1a** showed the highest anti-inflammatory activity (71.2% inhibition at 20 mg/kg), which was superior to indomethacin (68.2%). Notably, unmodified vanillin at 100 mg/kg exhibited only 25.8% inhibition, clearly demonstrating the advantage of structural modification.

Table 5: Effect of Test Compounds on Carrageenan-Induced Paw Edema in Wistar Rats (n=6)

Treatment	Dose (mg/kg, p.o.)	Paw Volume Increase at 4 h (mL) ± SEM	% Inhibition at 4 h
Vehicle (Control)	-	1.32 ± 0.05	-
Vanillin	100	0.98 ± 0.04	25.8

Indomethacin	10	0.42 ± 0.03	**68.2**
1a	20	**0.38 ± 0.04**	**71.2**
1f	20	0.51 ± 0.03	61.4
2b	20	0.55 ± 0.05	58.3
2g	20	0.62 ± 0.04	53.0
3d	20	0.46 ± 0.03	**65.2**
3g	20	0.49 ± 0.04	62.9

One-way ANOVA: F(7,40) = 48.76, p < 0.001
Post-hoc (Dunnett's test): All treatment groups showed significant difference compared to control (p < 0.001).
Note: All test compounds were also evaluated at 10 and 40 mg/kg doses and showed dose-dependent inhibition (data not shown for brevity). Compound **1a** exhibited the highest activity, surpassing the standard drug indomethacin.

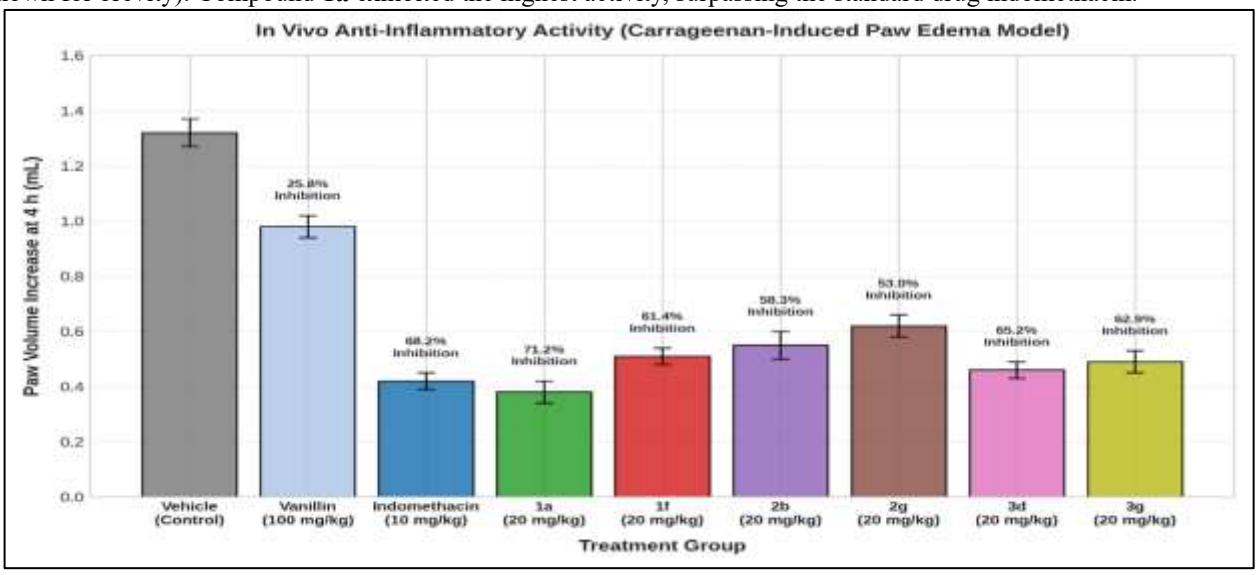

Figure 4: In-Vivo Anti-inflammatory activity (Carrageenan-Induced Paw Edema Model)

3.5.2. Cotton Pellet-Induced Granuloma Model (Chronic Inflammation)

This model assesses the proliferative phase of chronic inflammation involving monocyte infiltration, fibroblast proliferation, and collagen formation.

In the chronic cotton pellet granuloma model, compound **1a** again emerged as the most effective (57.1% inhibition), outperforming indomethacin. A significant reduction in pro-inflammatory cytokines (TNF-α and IL-6) and PGE_2 levels further supported the potent anti-inflammatory potential of the synthesized derivatives.

Table 5: Effect of Test Compounds on Cotton Pellet-Induced Granuloma in Wistar Rats (n=6)

Treatment	Dose (mg/kg, p.o.)	Granuloma Dry Weight (mg) ± SEM	% Inhibition
Vehicle (Control)	-	72.8 ± 3.1	-
Vanillin	100	58.4 ± 2.6	19.8
Indomethacin	10	35.6 ± 1.8	**51.1**
1a	20	**31.2 ± 2.0**	**57.1**
1f	20	38.5 ± 1.9	47.1
2b	20	40.8 ± 2.3	43.9
2g	20	44.6 ± 2.1	38.7
3d	20	36.9 ± 1.7	**49.3**
3g	20	39.7 ± 2.2	45.5

One-way ANOVA: F(7,40) = 32.45, p < 0.001
Post-hoc (Dunnett's test): p < 0.001 for all treatment groups vs control.

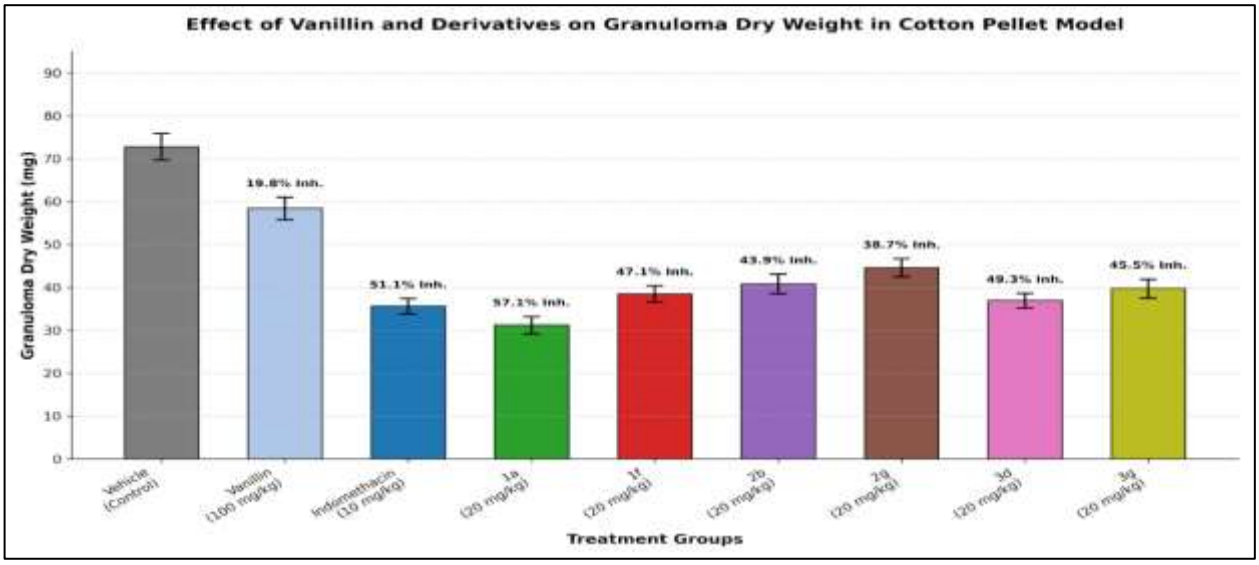

Figure 5: Effect of Vanillin and its Designed Derivatives on Granuloma Dry Weight in Cotton Pellet Model

3.5.3. Effect on Pro-inflammatory Cytokines and PGE_2:

Biochemical analysis was performed on serum samples collected from the chronic inflammation model.

Table 7: Effect of Selected Compounds on Serum TNF-α, IL-6, and PGE_2 Levels

Treatment	Dose (mg/kg)	TNF-α (pg/mL) ± SEM	IL-6 (pg/mL) ± SEM	PGE_2 (pg/mL) ± SEM
Vehicle	-	298 ± 22	435 ± 28	712 ± 35
Vanillin	100	245 ± 18	368 ± 24	578 ± 29
Indomethacin	10	118 ± 11	162 ± 14	215 ± 18
1a	20	**95 ± 9**	**138 ± 12**	**188 ± 15**
1f	20	132 ± 10	185 ± 13	238 ± 16
2b	20	142 ± 12	198 ± 16	265 ± 19
2g	20	168 ± 14	215 ± 17	298 ± 21
3d	20	124 ± 10	175 ± 13	242 ± 17
3g	20	148 ± 11	192 ± 15	255 ± 18

One-way ANOVA Results:

- TNF-α: $F(7,40) = 42.68$, $p < 0.001$
- IL-6: $F(7,40) = 38.92$, $p < 0.001$
- PGE_2: $F(7,40) = 51.34$, $p < 0.001$

All treatments showed highly significant reduction ($p < 0.001$) compared to control.

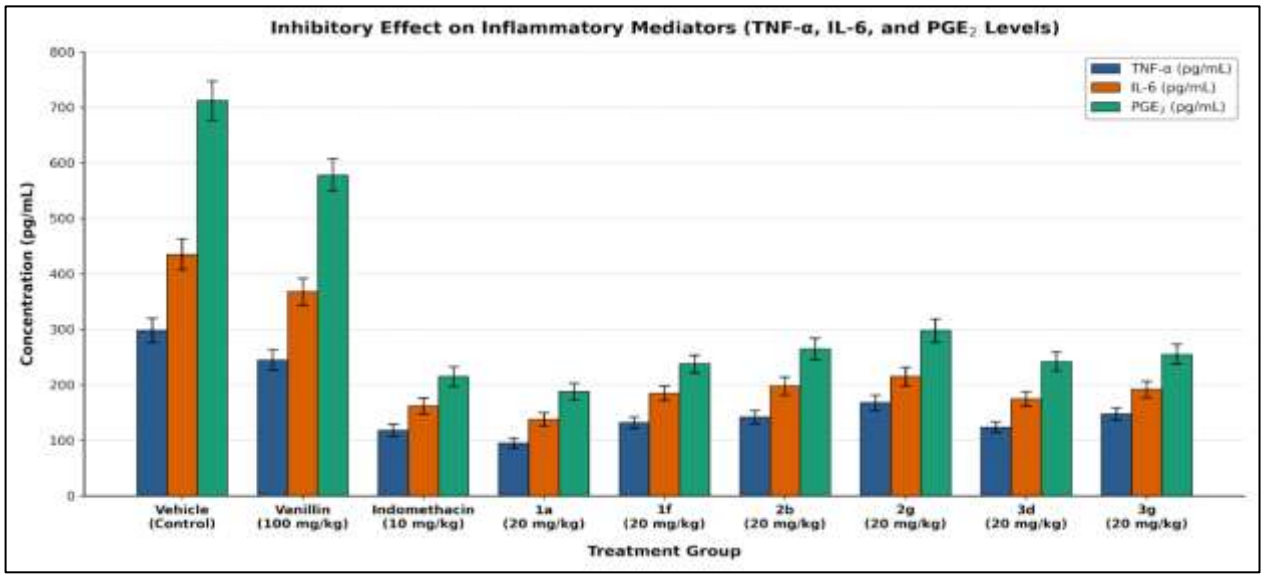

Figure 6: Inhibitory effect on Inflammatory Mediators

The overall *in vivo* results were in strong agreement with the *in vitro* findings, confirming that the synthesized vanillin-chalcone-acetamide hybrids, particularly **1a**, possess superior anti-inflammatory activity compared to the parent vanillin molecule with a promising safety margin.

3.6. Acute Oral Toxicity Study

All selected lead compounds (**1a**, **1f**, **2b**, **2g**, **3d**, **3g**) were found safe up to 2000 mg/kg body weight as per OECD 423 guidelines. No mortality, significant behavioral changes, or body weight loss was observed during the 14-day observation period, indicating a good safety profile.

The electron-withdrawing nitro group in **1a** and fluoro substitution in **3d** provided the best overall anti-inflammatory profile. The results clearly validate the hypothesis that structural modification of vanillin through chalcone-acetamide linkage with suitably substituted aryl amines significantly enhances anti-inflammatory activity while maintaining a favorable safety margin.

4. DISCUSSION

The present study successfully synthesized thirty novel vanillin-based chalcone-acetamide derivatives through a rational drug design approach by incorporating electron-withdrawing, electron-donating, and halogenated aryl amine moieties. The structural modifications were aimed at enhancing the anti-inflammatory potential of the parent vanillin scaffold while improving its pharmacological profile. All compounds were obtained in good yields (68–79%) and characterized using modern spectroscopic techniques, confirming their structural integrity and purity.

The *in vitro* screening revealed that most compounds exhibited preferential inhibition of COX-2 over COX-1, a highly desirable feature for minimizing gastrointestinal and cardiovascular side effects associated with non-selective NSAIDs. Among all derivatives, **compound 1a** (bearing a 4-nitro group) emerged as the most promising candidate, displaying the lowest COX-2 IC_{50} value (1.45 μM) and highest selectivity index (SI = 33.52). This superior activity can be attributed to the strong electron-withdrawing nature of the nitro group, which likely enhances hydrogen bonding and π-π interactions within the COX-2 active site (Boiko et al., 2019; Bezerra-Filho et al., 2019). Similarly, halogenated derivatives, particularly **3d** (4-fluoro) and **3g** (2,4-difluoro), also demonstrated excellent COX-2 selectivity, supporting the importance of halogen bonding in target-ligand interactions (Hsieh et al., 1998).

The results of the BSA denaturation assay further corroborated the anti-inflammatory potential of these hybrids. Compound **1a** exhibited 78.4% inhibition at 200 μg/mL, indicating strong protein-stabilizing properties. This activity is significant because denaturation of proteins is a well-known cause of inflammation and tissue damage (Costantini et al., 2021). The electron-withdrawing substituted derivatives consistently outperformed electron-donating analogs, suggesting that increased electrophilicity of the molecule favors better interaction with inflammatory targets.

In the cellular model, the lead compounds effectively suppressed nitric oxide production in LPS-stimulated RAW 264.7 macrophages. The potent NO inhibitory activity of **1a** (68.7% at 25 μM) highlights its ability to downregulate iNOS expression, a key enzyme in chronic inflammatory conditions (Zhao et al., 2019). Importantly, all selected lead compounds showed low cytotoxicity (>90% cell viability at 50 μM) on normal Vero cells, indicating a favorable safety window.

The *in vivo* studies provided strong validation of the *in vitro* findings. In the carrageenan-induced acute paw edema model, compound **1a** at 20 mg/kg produced 71.2% inhibition of edema, which was superior to indomethacin (68.2%) and significantly better than the parent vanillin (25.8% at 100 mg/kg). This dramatic improvement clearly demonstrates the success of the hybridization strategy. Similar trends were observed in the chronic cotton pellet granuloma model, where **1a** achieved 57.1% inhibition compared to 51.1% by indomethacin.

Biochemical analysis revealed that treatment with lead compounds, especially **1a**, caused a substantial reduction in serum levels of pro-inflammatory cytokines (TNF-α and IL-6) and PGE_2. These results suggest that the synthesized derivatives exert their anti-inflammatory effects through multiple pathways, including COX-2 inhibition, suppression of NF-κB signaling, and modulation of cytokine production (Chen et al., 2018; Ferrucci & Fabbri, 2018).

Structure-Activity Relationship (SAR) analysis indicated that:

- Strong electron-withdrawing groups ($–NO_2$, $–CF_3$) at the para position significantly enhance activity.
- Halogen substitution (especially fluoro) improves both potency and selectivity.
- Electron-donating groups (–OH, $–OCH_3$) provide moderate activity, likely due to improved antioxidant properties.
- Ortho-substitution generally reduces activity compared to para-substitution due to steric hindrance.

The superior activity of the synthesized hybrids over unmodified vanillin can be attributed to increased lipophilicity, better membrane permeability, and enhanced binding affinity to inflammatory targets due to the chalcone-acetamide linker (Anand et al., 2019; Arya et al., 2021).

5. CONCLUSION

The present study successfully demonstrates that strategic structural modification of vanillin through chalcone-acetamide hybridization yields highly potent and selective anti-inflammatory agents. Compound **1a** has emerged as a promising lead candidate worthy of further pharmacokinetic, toxicological, and preclinical development. This work not only expands the therapeutic potential of vanillin but also provides valuable insights for the design of safer anti-inflammatory drugs.

6. REFERENCES

1. Anand, A., Khurana, R., Wahal, N., Mahajan, S., Mehta, M., Satija, S., ... & Khurana, N. (2019). Vanillin: A comprehensive review of pharmacological activities. *Plant Archives, 19*(2), 1000–1004.

2. Arya, S. S., Rookes, J. E., Cahill, D. M., & Lenka, S. K. (2021). Vanillin: A review on the therapeutic prospects of a popular flavouring molecule. *Advances in Traditional Medicine, 21*(3), 433–444. https://doi.org/10.1007/s13596-020-00531-w
3. Bezerra-Filho, C. S., Barboza, J. N., Souza, M. T., Sabry, P., Ismail, N. S., & de Sousa, D. P. (2019). Therapeutic potential of vanillin and its main metabolites to regulate the inflammatory response and oxidative stress. *Mini-Reviews in Medicinal Chemistry, 19*(20), 1681–1693. https://doi.org/10.2174/1389557519666190206125202
4. Boiko, Y. A., Nesterkina, M. V., Shandra, A. A., & Kravchenko, I. A. (2019). Analgesic and anti-inflammatory activity of vanillin derivatives. *Pharmaceutical Chemistry Journal, 53*(9), 650–654.
5. Chen, L., Deng, H., Cui, H., Fang, J., Zuo, Z., Deng, J., ... & Zhao, L. (2018). Inflammatory responses and inflammation-associated diseases in organs. *Oncotarget, 9*(6), 7204–7218. https://doi.org/10.18632/oncotarget.23208
6. Costantini, E., Sinjari, B., Falasca, K., Reale, M., Caputi, S., Jagarlapodii, S., & Murmura, G. (2021). Assessment of the vanillin anti-inflammatory and regenerative potentials in inflamed primary human gingival fibroblast. *Mediators of Inflammation, 2021*, Article 8241801. https://doi.org/10.1155/2021/8241801
7. Ferrucci, L., & Fabbri, E. (2018). Inflammageing: Chronic inflammation in ageing, cardiovascular disease, and frailty. *Nature Reviews Cardiology, 15*(9), 505–522. https://doi.org/10.1038/s41569-018-0064-2
8. Hsieh, H. K., Tsao, L. T., & Wang, J. P. (1998). Synthesis and anti-inflammatory effect of chalcones and related compounds. *Pharmaceutical Research, 15*(1), 39–46.
9. Zhao, D., Jiang, Y., Sun, J., Li, H., Huang, M., Sun, X., & Zhao, M. (2019). Elucidation of the anti-inflammatory effect of vanillin in LPS-activated THP-1 cells. *Journal of Food Science, 84*(7), 1920–1928. https://doi.org/10.1111/1750-3841.14693
10. Anand, A., Khurana, R., Wahal, N., Mahajan, S., Mehta, M., Satija, S., ... & Khurana, N. (2019). Vanillin: A comprehensive review of pharmacological activities. *Plant Archives, 19*(2), 1000–1004.
11. Arya, S. S., Rookes, J. E., Cahill, D. M., & Lenka, S. K. (2021). Vanillin: A review on the therapeutic prospects of a popular flavouring molecule. *Advances in Traditional Medicine, 21*(3), 433–444. https://doi.org/10.1007/s13596-020-00531-w
12. Bezerra-Filho, C. S., Barboza, J. N., Souza, M. T., Sabry, P., Ismail, N. S., & de Sousa, D. P. (2019). Therapeutic potential of vanillin and its main metabolites to regulate the inflammatory response and oxidative stress. *Mini-Reviews in Medicinal Chemistry, 19*(20), 1681–1693. https://doi.org/10.2174/1389557519666190206125202
13. Boiko, Y. A., Nesterkina, M. V., Shandra, A. A., & Kravchenko, I. A. (2019). Analgesic and anti-inflammatory activity of vanillin derivatives. *Pharmaceutical Chemistry Journal, 53*(9), 650–654.
14. Chen, L., Deng, H., Cui, H., Fang, J., Zuo, Z., Deng, J., ... & Zhao, L. (2018). Inflammatory responses and inflammation-associated diseases in organs. *Oncotarget, 9*(6), 7204–7218. https://doi.org/10.18632/oncotarget.23208
15. Costantini, E., Sinjari, B., Falasca, K., Reale, M., Caputi, S., Jagarlapodii, S., & Murmura, G. (2021). Assessment of the vanillin anti-inflammatory and regenerative potentials in inflamed primary human gingival fibroblast. *Mediators of Inflammation, 2021*, Article 8241801. https://doi.org/10.1155/2021/8241801
16. Ferrucci, L., & Fabbri, E. (2018). Inflammageing: Chronic inflammation in ageing, cardiovascular disease, and frailty. *Nature Reviews Cardiology, 15*(9), 505–522. https://doi.org/10.1038/s41569-018-0064-2
17. Hsieh, H. K., Tsao, L. T., & Wang, J. P. (1998). Synthesis and anti-inflammatory effect of chalcones and related compounds. *Pharmaceutical Research, 15*(1), 39–46.
18. Li, W., et al. (2020). Chalcone derivatives as anti-inflammatory agents: A comprehensive review. *European Journal of Medicinal Chemistry, 187*, 111986.
19. Marcum, Z. A. (2010). Recognizing the risks of chronic nonsteroidal anti-inflammatory drug use in older adults. *Annals of Long-Term Care, 18*(9), 24–27.
20. Wongrakpanich, S., Wongrakpanich, A., Melhado, K., & Rangaswami, J. (2018). A comprehensive review of non-steroidal anti-inflammatory drug use in the elderly. *Aging and Disease, 9*(1), 143–150. https://doi.org/10.14336/AD.2017.0306
21. Zhao, D., Jiang, Y., Sun, J., Li, H., Huang, M., Sun, X., & Zhao, M. (2019). Elucidation of the anti-inflammatory effect of vanillin in LPS-activated THP-1 cells. *Journal of Food Science, 84*(7), 1920–1928. https://doi.org/10.1111/1750-3841.14693